International Journal of Applied Electromagnetics and Mechanics 15 (2001/2002) 409–416
IOS Press

Magnetic domain dynamics visualization

Hisashi Endo[a,*], Seiji Hayano[a], Masahiro Fujikura[b], Hisashi Mogi[b], Chikara Kaido[c] and Yoshifuru Saito[a]
[a]*Graduate School of Engineering, Hosei University, 3-7-2 Kajino, Koganei, 184-8584 Tokyo, Japan*
[b]*Steel Products Lab.-1, Steel Research Lab., Nippon Steel Co., 20-1 Shintomi, Futtsu, 293-8511 Chiba, Japan*
[c]*Yawata R & D Lab., Nippon Steel Co., 1-1 Tobihata, Tobata, Kitakyushu, 804-8501 Fukuoka, Japan*

Abstract. This paper proposes a visualizing methodology of iron loss generation in a magnetic material using its visualized domain images, i.e., SEM, Kerr and Faraday effects. Based on the differential equations for dynamic image, the material behavior is visualized. The state transition matrix of the Helmholtz equation, for which is derived from a series of distinct visualized domain images representing magnetized state. This makes it possible to visualize the magnetizing mechanism as well as iron loss generation. In the present paper, visualization of iron loss generation on a grain-oriented electrical steel sheet is worked out using a set of SEM images. As a result of our image analysis, magnetization curves at the particular points can be estimated.

1. Introduction

Controlling the magnetized condition of electrical steels is very important to the design of efficient electrical devices with high efficiency. In case of grain oriented electrical steels, the tilt angle of the $<001>$ axis from the surface of the specimen (the tilt angle β) must be zero to prevent generating closure domains causing eddy current loss. The understanding of domain structure and motion leads to the evaluation of iron loss [1]. Heretofore elaborate analysis and/or simulators could only accomplish such a task. The aim of the present study is to provide a simple means to visualize and to evaluate the domain motion dynamics of the grain oriented electrical steels.

In the present paper, we propose a novel image analysis approach using scanning electron microscope (SEM) images. Previously, magnetization reversal dynamics in magnetic thin films has been reported using the magneto-optical microscope magnetometer [2,3]. In case of electrical steels, we must take into account the structure in depth of the specimen to clarify the lancet domain generation. Therefore, we employ SEM imaging.

To analyze our SEM images we employ the image Helmholtz equation method which enables us to extract the characteristics of the dynamic system from the finite number of visualized images. The characteristics of the domain motion can be deduced from the state transition matrix of the image Helmholtz equation [4].

As a result of this analysis, domain motion and iron loss can be evaluate from the elements in the state transition matrix. The physical meaning of the elements constituting the state transition matrix is obtained by relating them to the Preisach distribution functions. In this methodology, magnetization curve as well as domain images are generated as solutions to the image Helmholtz equation.

*Corresponding author: Hisashi Endo, Graduate School of Engineering, Hosei University, 3-7-2 Kajino, Koganei, Tokyo 184-8584, Japan. Tel.: +81 42 387 6200; Fax: +81 42 387 6200; E-mail: endo@ysaitoh.k.hosei.ac.jp.

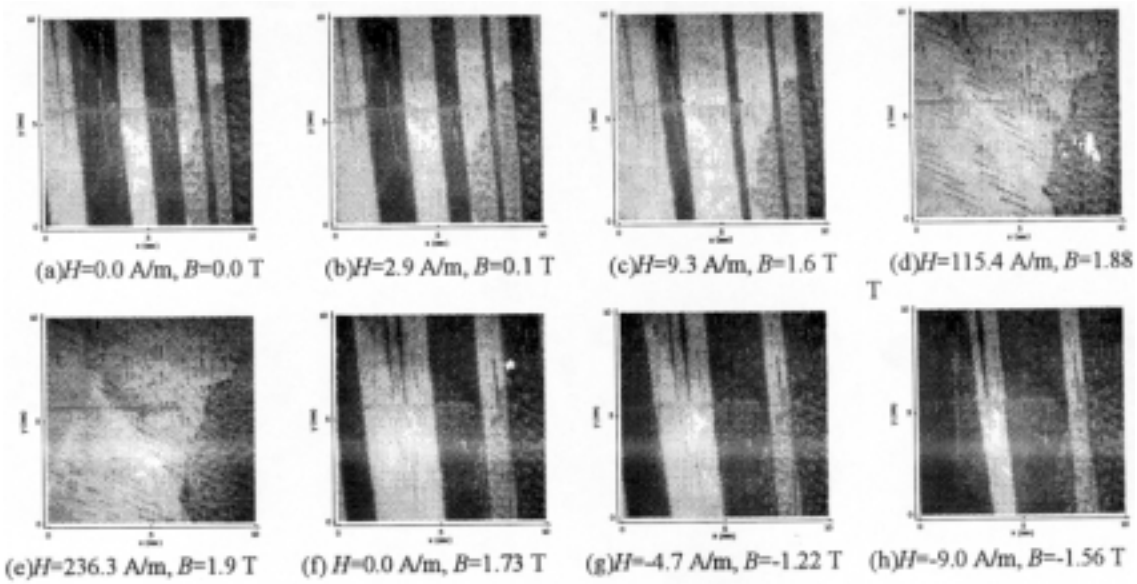

Fig. 1. Magnetic domain SEM images of the ORIENTCORE HI-B produced by Nippon Steel Co. (100×100 pixels, 0.1 mm/pixel).

Table 1
Measured Domain Images

Image No.	H (A/m)	B (T)	Image No.	H (A/m)	B (T)
1	0.00	0.00	13	214.13	1.93
2	2.85	0.10	14	160.37	1.91
3	9.26	1.63	15	98.68	1.91
4	24.16	1.73	16	54.66	1.84
5	30.23	1.78	17	28.53	1.83
6	54.59	1.84	18	3.73	1.77
7	84.92	1.86	19	0.00	1.73
8	115.39	1.88	20	−4.60	1.73
9	160.69	1.90	21	−5.95	−0.06
10	236.32	1.92	22	−7.45	−1.43
11	324.31	1.95	23	−9.07	−1.56
12	269.64	1.95	24	−11.50	−1.62

H: External magnetic field intensity, B: Flux density

2. Domain motion analysis

2.1. Domain images of a grain oriented electrical steel sheet

A lot of domain observation techniques are available, e.g., Kerr effect and electron microscopies. The thickness of electrical steels becomes 10^{-4} mm order. In such a case, SEM observation is useful way from a viewpoint of practical use. Figure 1 shows the magnetic domain images of a grain oriented electrical steel under the distinct magnetized states [5]. The specimen is the ORIENTCORE HI-B produced by Nippon Steel Corporation and its thickness is 0.23 mm. The observation was carried out using SEM accelerated to 160 kV. Table 1 lists the domain images used in this paper.

2.2. Image helmholtz equation

To extract the characteristics of domain motion from given SEM images, we employ the image Helmholtz equation method [4]. In this method, a domain image is composed of a scalar field U, and then the dynamics of domains motion can be represented by the image Helmholtz equation [6]. In a magnetized state, applied field H causes domain motion, so that our image Helmholtz equation is reduced into:

$$\nabla^2 U + \varepsilon \frac{\partial}{\partial \alpha} U = -\sigma, \tag{1}$$

where ε and σ respectively denote a domain motion parameter and an image source density given by the Laplacian of a final domain image U_{Final}. The first and second terms on the left in Eq. (1) represent the spatial expanse and transition of image to the field H, respectively. In Eq. (1), the parameter ε is not given. Key idea of our method is to determine the ε from SEM images.

2.3. Solution of the image helmholtz equation

The modal analysis to Eq. (1) gives a general solution:

$$U(H) = \exp\left(-\Lambda H\right)(U_{\mathrm{Start}} - U_{\mathrm{Final}}) + U_{\mathrm{Final}}, \tag{2}$$

where U_{Start} and $\exp\left(-\Lambda H\right)$ are an initial image and a state transition matrix, respectively. The values ε and σ in Eq. (1) are respectively reduced into the matrix Λ and final image U_{Final}. Because of the parameter ε in Eq. (1), the state transition matrix is unknown. Equation (2) generates the initial image UStart if $H = 0$, and the final image U_{Final} when the variable H reaches to infinity. Actually, H never reaches infinity so that it is necessary to determine the matrix Λ from the given domain images.

2.4. Determination of the matrix Λ

If we have the solution $U(H)$ in Eq. (2), then it is possible to determine the elements in matrix Λ by taking logarithm, as given by

$$\Lambda = -\frac{1}{H} \ln\left(\frac{U(H) - U_{\mathrm{Final}}}{U_{\mathrm{Start}} - U_{\mathrm{Final}}}\right). \tag{3}$$

Discretizing Eq. (3) to the applied field, the elements in the i-th matrix Λ_i can be determined from a series of three distinct domain images viz,

$$\Lambda_i = -\frac{1}{H_{i+1} - H_i} \ln\left(\frac{U_{i+1} - U_{i+2}}{U_i - U_{i+2}}\right), \quad i = 1, 2, \ldots, 22. \tag{4}$$

The subscript i of U in Eq. (4) refers to a domain image numbered in Table 1. Moreover, U_i and U_{i+2} correspond to U_{Start} and U_{Final} in Eq. (2), respectively. Therefore, it is possible to analytically generate a domain image by substituting Λ_i into Eq. (2).

2.5. Physical meaning of the elements constituting the matrix Λ

If the domain motion can be represented by the parameter ε in Eq. (1), then the transition information between the initial and the final domain images can be represented by the state transition matrix. The matrix Λ is composed of complex numbers. As is well known in control theory, the real and imaginary parts represent in phase and 90-degree difference phase components to the excitation H, respectively. Therefore, observing the elements in the imaginary part of the matrix Λ leads to identification of iron loss generating parts.

Saito, Hayano, and Sakaki have recently reported a theoretical model of magnetic materials exhibiting hysteric behavior. They derived following constitutive equation [7,8]:

$$B + \frac{\mu}{\Psi}\frac{\partial B}{\partial H} = \mu H + \frac{\mu\mu_r}{\Psi}, \tag{5}$$

where μ and μ_r are the permeability and reversal permeability, respectively. Moreover, Ψ denotes the Preisach distribution function. If the scalar potential U in Eq. (1) is taken to be the flux density B in Eq. (5), then the parameter ε in Eq. (1) is related to the reciprocal of Preisach's function in dimension. Let the reversing and applying point field intensities be defined as H_n and H_p, respectively. Then Preisach's function can be represented by

$$\Psi = \frac{\partial^2 B}{\partial H_p \partial H_n}. \tag{6}$$

The function Ψ is then the rate of change of permeability to the applied field H [9]. Therefore, our visualization also suggests a magnetization parameter determination from microscopically observed domain images. Since the elements in the matrix Λ should be constant values, then this approximation method is only applicable to small $\mathrm{d}B/\mathrm{d}H$ region.

3. Visualization of domain motion dynamics

3.1. Iron loss visualization by means of matrix Λ

Figure 2 shows the real and imaginary elements in matrix Λ along with the domain pattern in Fig. 1. Consider the real parts of the matrices Λ in Fig. 2. In a small field, the moving parts of the negatively magnetized parts (black parts in Fig. 1) become zero. This means that this magnetization process is mainly carried out by the magnetic boundary displacements (real part of Fig. 2(a)) and magnetic domain movements (real part of Fig. 2(b)). Increasing the field, the values in Λ represent corresponding to the rotation of magnetization (real part of Fig. 2(c)). As seen in Eq. (6), Λ taking a small in value in the real and imaginary parts suggest that the rate of change of permeability to the applied field H is small so that such a process is linear in the applied field. Conversely, a large value of Λ means that the rate of change of permeability to the applied field becomes large and result in non-linear magnetization processes. Second, consider the imaginary parts of matrices Λ in Fig. 2. In a small field, the real part of this region corresponds to the magnetic boundary displacement. However, in case of imaginary part, the elements in Λ are close to zero (imaginary part of Fig. 2(a)). This means that the magnetic boundaries move without delay components. In the right side of Fig. 2(b), the values represent at the grain boundary. This is considered to be the force against the applied field. Increasing the field results in the generation of lancet domains (imaginary part of Fig. 2(c)). In this region, these matrix elements are then related to iron loss.

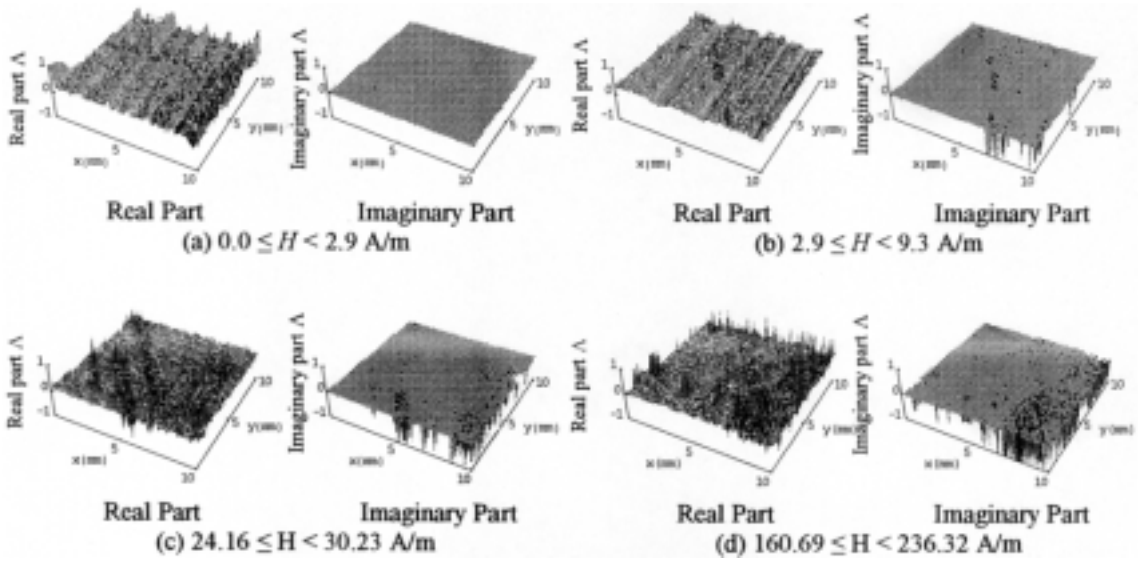

Fig. 2. State transition matrices.

3.2. Domain image reconstruction and magnetization curve

The contrast of SEM images shown in Fig. 1 corresponds to the polarity of magnetization. A summation of all magnetization gives a flux density in a magnetic material. Computing an average of pixel value on entire domain image just corresponds to a flux density in a magnetic material.

Figure 3 shows the computed magnetization curve. Since Eq. (2) is possible to generate the domain images analytically, then the smooth computed magnetization curve is generated. Even though the domain images represent a limited area of the specimen, we have good agreement with the experimental result as shown in Fig. 4.

3.3. Magnetization curves at the particular points

When we focus on a magnetization curve at a particular point on the domain image, it is possible to draw the local magnetization curves. In order to demonstrate the local magnetization curves, Fig. 5(a) shows the selected sample positions depending on the physical differences. The features of the selected positions in Fig. 5(a) are as follows.

- Position Nos. 1 and 2: At the 180° domains
- Position Nos. 3 and 4: At the lancet domains
- Position Nos. 5 and 6: At the strained parts

Figures 5(b)–(d) show the magnetization curves computed from each of the pixel values. At first, in the magnetization curves at the 180° basic domains (Fig. 5(b)), the residual inductions are higher than those at the lancet domains (Fig. 5(c)) and the strained parts (Fig. 5(d)). This means that the lancet and strained parts are hard to be magnetized. Inversely, the 180° basic domains are hard to move due to keeping minimum static magnetic energy. Second, in Fig. 5(c), the discontinuous curves are obtained at the beginning of rotating magnetization region due to the lancet domain generations. This result is corresponding well to supporting [10]. Finally, in Fig. 5(d), a discontinuous curve is obtained at the position 5 due to the physical stress to the specimen. However, the curve at the position 6 is reconstructed smoothly. This may be considered to cause by stretching strain.

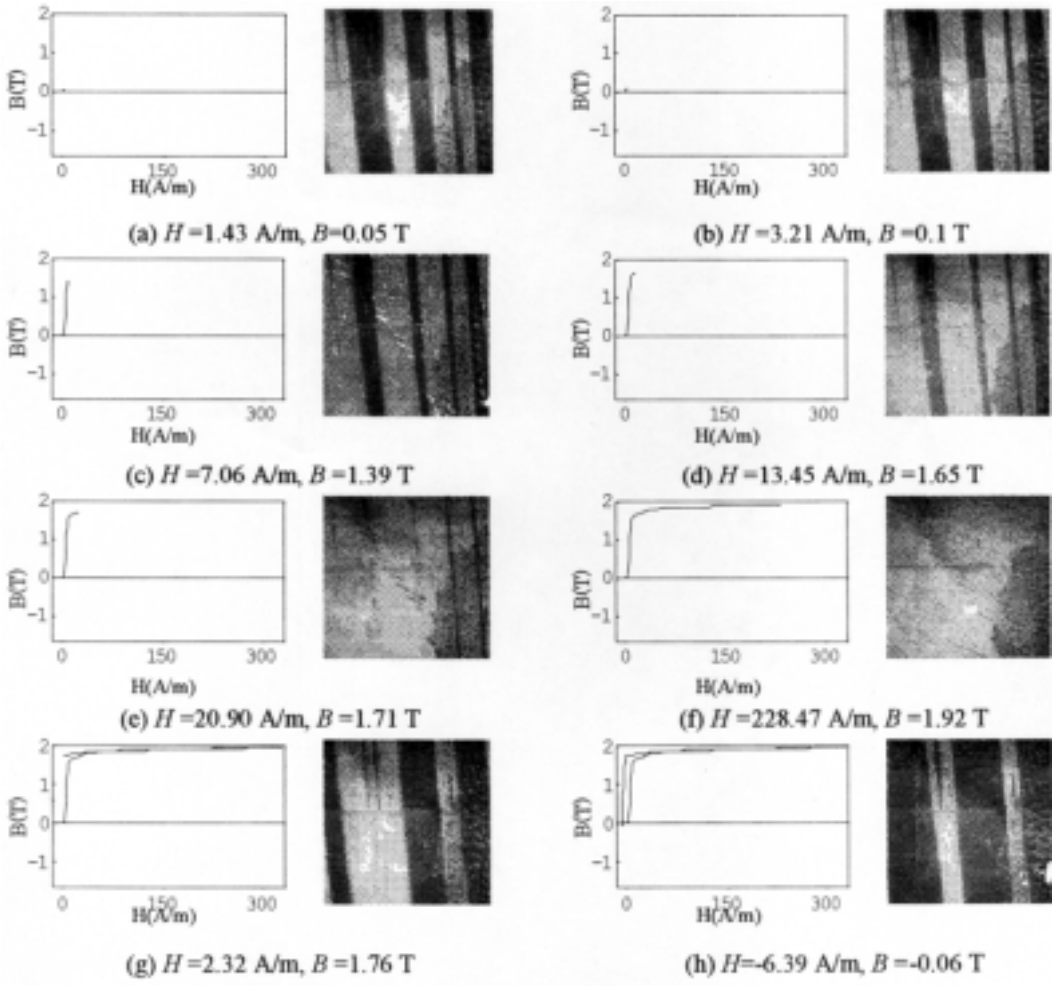

Fig. 3. Reconstructed domain patterns and magnetization curves.

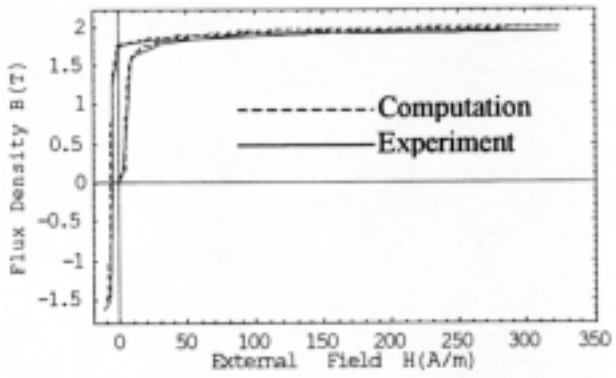

Fig. 4. Comparison computation with experiment.

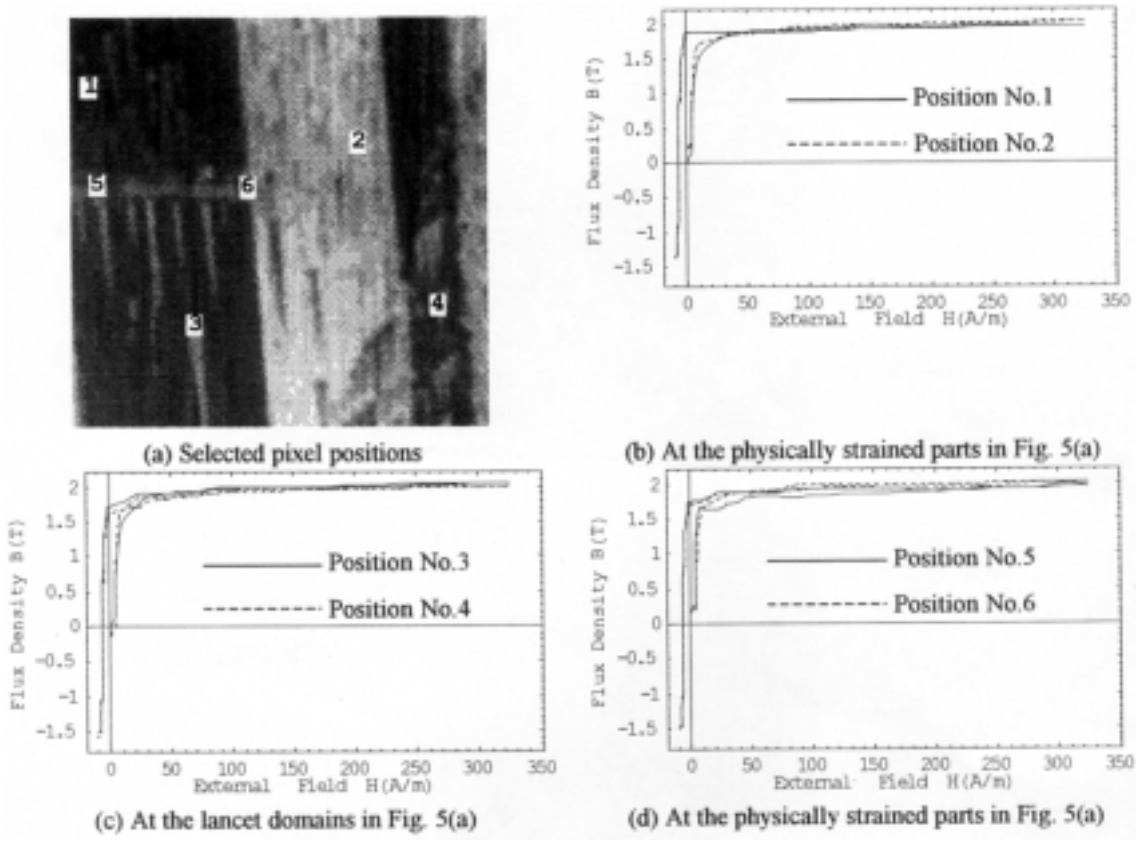

Fig. 5. Magnetization curves at the particular points.

4. Conclusions

We have proposed a method of determining magnetization dynamics and iron loss using visualized domain images. State transition matrices derived from a series of distinct SEM domain images are used to the behavior of magnetic domains in the iron loss generating parts. In highly magnetized region of electrical steels, the rotation of magnetization causes small domains on the surface of the specimen because of the tilt angle β [10]. Then, this effect causes closure domain generation resulting in iron loss. Our analysis based on the matrix Λ clearly reproduces experimental observation. Second, the magnetized domain images and the magnetization curve can be reproduced by the solution of the image Helmholtz equation. Even though only a small number of images are given, the magnetization curves can be generated reflecting on the domain physical situations by our method. Therefore, our method is capable of providing both microscopic and macroscopic material parameters.

References

[1] Hubert and R. Schäfer, *Magnetic Domains, Springer*, Berlin, 2000.
[2] J.-P. Jamet et al., Dynamics of the magnetization reversal in Au/Co/Au micrometer-size dot arrays, *Phys. Rev. B* **57**(22) (1998), 14320–14331.

[3] S.-B. Choe and S.-C. Shin, Magnetization reversal dynamics with submicron-scale coercivity variation in ferromagnetic films, *Phys. Rev. B* **62**(13) (2000), 8646–8649.
[4] H. Endo, S. Hayano, Y. Saito and T.L. Kunii, A method of image processing and its application to magnetodynamic fields, *Trans. IEE of Japan* **120-A**(10) (in Japanese) (2000), 913–918.
[5] T. Nozawa, T. Yamamoto, Y. Matsuo and Y. Ohya, Effects of scratching on losses in 3-percent Si-Fe single crystals with orientation near (110)[001], *IEEE Trans. Magn.* **15**(2) (1979), 972–981.
[6] H. Endo, S. Hayano, Y. Saito and T. L. Kunii, Image governing equations and its application to vector fields, *Trans. IEE of Japan* **120-A**(12) (in Japanese) (2000), 1089–1094.
[7] Y. Saito, S. Hayano and Y. Sakaki, A parameter representing eddy current loss of soft magnetic materials and its constitutive equation, *J. Appl. Phys.* **64**(1) (1988), 5684–5686.
[8] Y. Saito, K. Fukushima, S. Hayano and N. Tsuya, Application of a Chua type model to the loss and skin effect calculation, *IEEE Trans. Magn.* **23**(5) (1987), 2227–2229.
[9] L. Liorzou, B. Phelps and D. L. Atherton, Macroscopic models of Magnetization, *IEEE Trans. Magn.* **36**(2) (2000), 418–427.
[10] Kaido et al., *A discussion of the magnetic properties of non-oriented steel sheets*, Workshop of IEE of Japan, in Japanese, MAG-99-173, 1999.